Dyes and Pigments 92 (2012) 1370–1375

Contents lists available at SciVerse ScienceDirect

Dyes and Pigments

journal homepage: www.elsevier.com/locate/dyepig

A selective fluorescent chemosensor with 1, 2, 4-triazole as subunit for Cu (II) and its application in imaging Cu (II) in living cells

Jun Zhang*, Chunwei Yu, Shiyun Qian, Gang Lu, Jinlong Chen

School of Tropical and Laboratory Medicine, Hainan Medical University, Haikou 571101, China

ARTICLE INFO

Article history:
Received 9 September 2011
Accepted 22 September 2011
Available online 4 October 2011

Keywords:
Rhodamine derivative
Fluorescent chemosensors
Triazole
Metal ions
Fluorescence enhancement
Fluorescence imaging

ABSTRACT

A chemosensor based on rhodamine B with 1, 2, 4-triazole as subunit was synthesized and characterized. It exhibits high selectivity and sensitivity for Cu^{2+} in ethanol/water (6:4, v:v) of pH 7.0 HEPES buffer solution and undergoes ring opening mechanism, and a 2:1 metal–ligand complex is formed. The chemosensor displays a linear response to Cu^{2+} in the range between 1.0×10^{-7} M and 1.0×10^{-6} M with a detection limit of 4.5×10^{-8} M. Its capability of biological application was also evaluated and the results show that this chemosensor could be successfully employed as a Cu^{2+}-selective chemosensor in the fluorescence imaging of living cells.

1. Introduction

Detecting the presence of transition metal ions has received considerable attention, mostly because these metal ions play important roles in living systems and have an extremely ecotoxicological impact on the environment and human. Among the various transition metal ions, Cu^{2+} plays a critical role as a catalytic cofactor for a variety of metalloenzymes, including superoxide dismutase, cytochrome *c* oxidase and tyrosinase [1]. However, under overloading conditions, Cu^{2+} exhibits toxicity in that it causes neurodegenerative diseases, probably by its involvement in the production of reactive oxygen species [2]. Chemosensors based on ion-induced changes in fluorescence appear to be particularly attractive due to their simplicity, high sensitivity, high selectivity, and instantaneous response [3]. Therefore, numerous excellent studies focus on the design of fluorescent chemosensors and the analysis of Cu^{2+}. Most of the reported Cu^{2+} fluorescent chemosensors, however, generally undergo fluorescence quenching upon the binding of Cu^{2+} [4–10], which is not as sensitive as a fluorescence enhancement response. Therefore, the development of highly sensitive and selective "off–on" chemosensor for Cu^{2+} is necessary. Based on our previous research [11–13], it is necessary to choose an efficient fluorophore and consider the geometry of coordination sites for a certain cation. Herein, we describe a new and simple fluorescent Cu^{2+} chemosensor **L** based on the equilibrium between the spirolactam (non-fluorescence) and the ring-opened amide (fluorescence) of rhodamine derivatives. In chemosensor **L**, we chose the rhodamine derivative as the fluorophore due to its excellent photophysical properties, such as long wavelength absorption and emission, high fluorescence quantum yield, large extinction coefficient, and high stability against light [14]. In addition, to take advantage of the 1, 2, 4-triazole subunit containing lone electron pairs on N, the semirigid ligand could effectively chelate Cu^{2+} according to the ionic radius and limit the geometric structure of the complex. With this intention, a Cu^{2+}-specific fluorescent and colorimetric chemosensor **L** derived from rhodamine B with 1, 2, 4-triazole as subunit was designed and synthesized (Scheme 1).

2. Experimental

2.1. Reagents and instruments

All reagents and solvents are of analytical grade and used without further purification. The metal ions and anions salts employed are NaCl, $MgCl_2 \cdot 6H_2O$, $CdCl_2$, $HgCl_2$, $CaCl_2 \cdot 2H_2O$, $FeCl_3 \cdot 6H_2O$, $CrCl_3 \cdot 6H_2O$, $Zn(NO_3)_2 \cdot 6H_2O$, $AgNO_3$, $CoCl_2 \cdot 6H_2O$, $MnCl_2 \cdot 4H_2O$, $CuCl_2 \cdot 2H_2O$, $NiCl_2 \cdot 6H_2O$, $PbCl_2$, NaClO, $NaNO_3$, Na_2CO_3, NaCl, NaAc, $NaClO_4$, KBr and Na_2HPO_4, respectively.

Fluorescence emission spectra were conducted on a HORIBA Fluoromax-4 spectrofluometer. UV–vis spectra were obtained on a Beckman DU-800 spectrophotometer (USA). Nuclear magnetic

* Corresponding author. Tel.: +86 898 66973190; fax: +86 898 66989173.
E-mail address: jun_zh1979@163.com (J. Zhang).

0143-7208/$ – see front matter © 2011 Elsevier Ltd. All rights reserved.
doi:10.1016/j.dyepig.2011.09.020

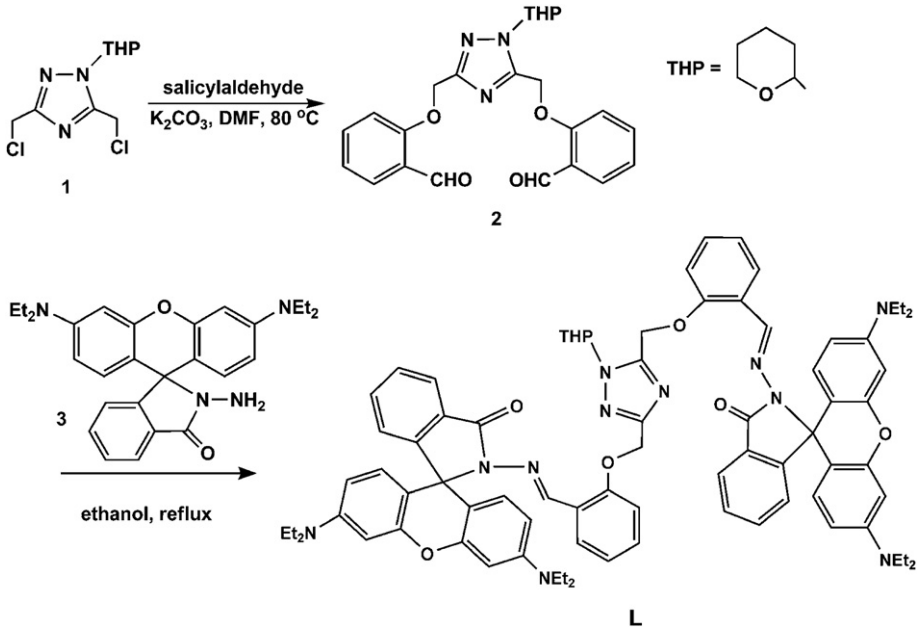

Scheme 1. Synthesis route of **L**.

resonance (NMR) spectra were measured with a Brucker WM-300 instrument and chemical shift were given in ppm from tetramethylsilane (TMS). Mass (MS) spectra were recorded on a Thermo TSQ Quantum Access Agillent 1100. Fluorescence imaging was performed by confocal fluorescence microscopy on an Olympus FluoView Fv1000 laser scanning microscope (USA). Melting points were taken on a WRS-1B digital melting-point apparatus.

2.2. Synthetic procedure

2.2.1. Synthesis of compound *2*

Compound **1** was synthesized as described before [15]. Under N_2 gas, salicylaldehyde (2.4 mmol) and Na_2CO_3 (4.0 mmol) were combined in DMF (40 mL) and stirred. Compound **1** (1.0 mmol) in DMF (10 mL) was added dropwise. The reaction mixture was stirred at 80 °C for 24 h, and then was poured into 500 mL cooled water, and the precipitate so produced was filtered off and recrystallized with ethanol to give **2** as white solid. Yields: 85.2%. M.p.: 116.1–117.2 °C. MS (ES+) *m/z*: 338.2 (M-THP+H^+). ^{1}H NMR (δ ppm, $CDCl_3$): 10.52 (s, 1H), 10.44 (s, 1H), 7.86 (t, 1H, J = 4.40 Hz), 7.74 (t, 1H, J = 4.40 Hz), 7.58 (d, 1H, J = 12.00 Hz), 7.54 (d, 1H, J = 12.00 Hz), 7.20 (s, 2H), 7.18 (s, 2H), 7.12 (t, 1H, J = 16.00 Hz), 7.06 (t, 1H, J = 16.00 Hz), 5.66 (d, 1H, J = 8.00 Hz) 5.43 (s, 2H), 5.27 (s, 2H), 4.00 (d, 1H, J = 12.00 Hz), 3.63 (d, 1H, J = 18.60 Hz), 2.32 (m, 1H, J = 16.00 Hz), 2.09 (m, 1H, J = 17.20 Hz), 1.99 (m, 1H, J = 10.00 Hz), 1.71 (m, 2H, J = 12.80 Hz), 1.62 (m, 2H, J = 18.40 Hz). ^{13}C NMR (δ ppm, $CDCl_3$): 189.78, 189.05, 160.84, 159.60, 158.25, 151.61, 135.97, 135.70, 129.30, 128.18, 125.44, 125.29, 122.06, 121.40, 113.37, 113.05, 85.02, 61.52,29.61, 24.59, 21.79, 67.67, 63.99.

2.2.2. Synthesis of compound *L*

Compound **3** was synthesized according to reported method [16]. Compound **2** (1.0 mmol) and compound **3** (2.2 mmol) were mixed in 30 mL ethanol and refluxed for 4 h. After cooling to room temperature, the precipitate so obtained was washed with water and ethanol, and then dried in vacuum. The **L** was obtained by recrystallization with ethanol as pale yellow solid. Yields: 75.3%. M.p.: 186.2–187.8 °C. MS (ES+) *m/z*: 1320.96 (M+Na^+). ^{1}H NMR (δ ppm, $CDCl_3$): ^{1}H NMR: 9.37 (s, 1H), 9.30 (s, 1H), 7.96 (s, 1H), 7.95 (s, 1H), 7.9 (d, 1H, J = 7.5 Hz), 7.76 (d, 1H, J = 6.55 Hz), 7.51 (d, 1H, J = 6.05 Hz), 7.48 (d, 1H, J = 1.60 Hz), 7.47 (s, 1H), 7.46 (d, 1H, J = 1.75 Hz), 7.44 (d, 1H, J = 7.25 Hz), 7.17 (d, 2H, J = 4.26 Hz), 7.13 (m, 2H, J = 6.69 Hz), 6.98 (s, 1H), 6.96 (s, 1H), 6.90 (t, 2H, J = 9.36 Hz), 6.87 (m, 1H, J = 3.35 Hz), 6.84 (m, 1H, J = 7.50 Hz), 6.52 (s, 1H), 6.50 (d, 2H, J = 1.85 Hz), 6.49 (d, 1H, J = 2.90 Hz), 6.44 (d, 1H, J = 2.35 Hz), 6.42 (m, 3H, J = 6.63 Hz), 6.24 (d, 2H, J = 8.16 Hz), 6.22 (d, 1H, J = 2.20 Hz), 5.55 (d, 1H, J = 10.86 Hz), 5.19 (s, 2H, J = 2.80 Hz), 5.03 (s, 2H, J = 2.65 Hz), 3.82 (d, 1H, J = 6.39 Hz), 3.54 (t, 1H, J = 11.37 Hz), 3.30 (m, 8H, J = 10.35 Hz), 2.21 (m, 1H, J = 12.33 Hz), 2.17 (d, 1H, J = 10.32 Hz), 1.95 (t, 1H, J = 7.90 Hz), 1.86 (d, 1H, J = 6.18 Hz), 1.62 (d, 1H, J = 12.00 Hz), 1.56 (m, 1H, J = 14.10 Hz), 1.12 (t, 12H, J = 14.85 Hz). ^{13}C NMR (δ ppm, $CDCl_3$): 164.56, 164.48, 158.87, 157.62, 156.34, 153.51, 153.47, 153.38, 152.01, 151.62, 151.33, 148.83, 148.78, 144.97, 144.15, 133.17, 132.99, 131.04, 130.63, 130.09, 130.05, 128.29, 128.11, 128.04, 126.62, 126.32, 125.20, 124.82, 124.04, 123.92, 123.23, 121.99, 121.44, 114.36, 113.44, 107.90, 107.84, 107.81, 106.51, 106.47, 98.01, 97.92, 84.51, 67.40, 66.32, 66.19, 64.92, 62.10, 58.46, 53.43, 44.31, 29.71, 29.48, 24.75, 21.77, 18.45, 12.56, 12.62.

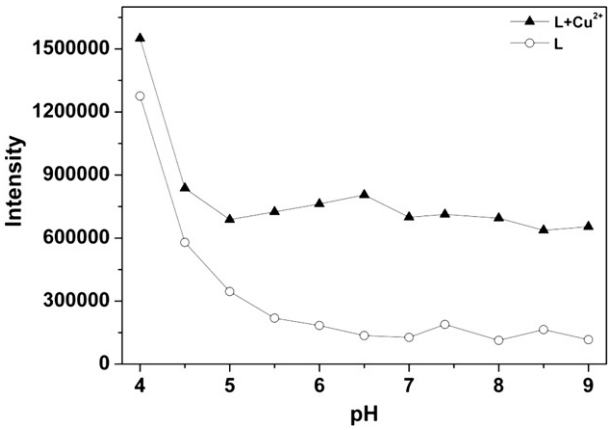

Fig. 1. Influences of pH on the fluorescence spectra of **L** (1.0 μM) (○) and **L** (1.0 μM) plus Cu^{2+} (50 μM) (▲) in ethanol–water solution (6:4, v:v). The pH was modulated by adding 1 M HCl or 1 M NaOH in HEPES buffers.

2.2.3. General spectroscopic methods

Metal ions and chemosensor **L** were dissolved in deionized water and DMSO to obtain 1 mM stock solutions, respectively. Before spectroscopic measurements, the solution was freshly prepared by diluting the high concentration stock solution to the corresponding solution.

2.2.4. Cell incubation

MCF-7 cells plated on coverslips were washed with phosphate-buffered saline (PBS), followed by incubating with 1 μM of $CuCl_2$ (in PBS) for 30 min at 37 °C, and then washed with PBS three times. After incubating with 20 μM of **L** for 30 min at 37 °C, the cells were washed with PBS three times again.

2.2.5. Cytotoxicity assay

Cytotoxicity in vitro was measured by using the methyl thiazolyl tetrazolium (MTT) assay in MCF-7 cells. Cells were seeded into 96-well cell culture plate at 4000/well, cultured at 37 °C and 5% CO_2 for 48 h, and then different concentrations of chemosensor **L** (0, 0.1, 1, 10 μM) were added to the wells. The cells were then incubated for 48 h at 37 °C under 5% CO_2. Subsequently, 20 μL MTT (5 mg/mL) was added to each well and incubated for an additional 4 h at 37 °C under 5% CO_2. Cells were lysed in triple liquid (10% SDS, 0.012 M HCl, 5% isopropanol), and the amount of MTT formazan was qualified by determining the absorbance at 570 nm using a microplate reader (Tecan, Austria).

The following formula was used to calculate the inhibition of cell growth: Cell viability (%) = (mean of Abs. value of treatment group/mean Abs. value of control) · 100%.

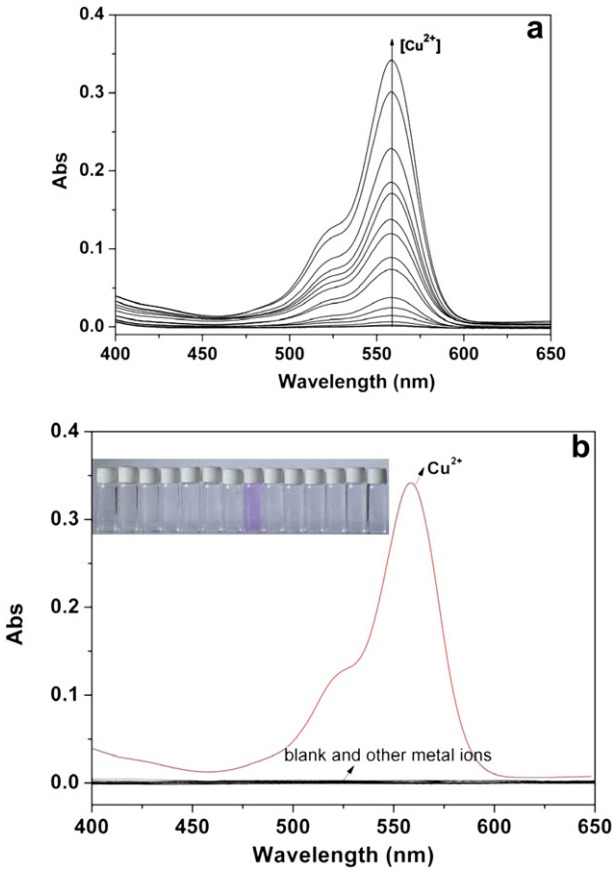

Fig. 2. (a) Absorbance spectra of **L** (10 μM) in ethanol–water solution (6:4, v:v. 50 mM HEPES, pH 7.0) in the presence of different amounts of Cu^{2+}. (b) UV–vis spectra of **L** (10 μM) with different metal ions (50 μM) in ethanol–water solution (6:4, v:v, 50 mM HEPES, pH 7.0). Inset: Change in color of **L** (20 μM) with metal ions (100 μM) (from left to right): blank, Ag^{+}, Ca^{2+}, Mg^{2+}, Zn^{2+}, Pb^{2+}, Fe^{3+}, Cu^{2+}, Cd^{2+}, Co^{2+}, Ni^{2+}, Mn^{2+}, Cr^{3+} and Hg^{2+}. (For interpretation of the references to color in this figure legend, the reader is referred to the web version of this article.)

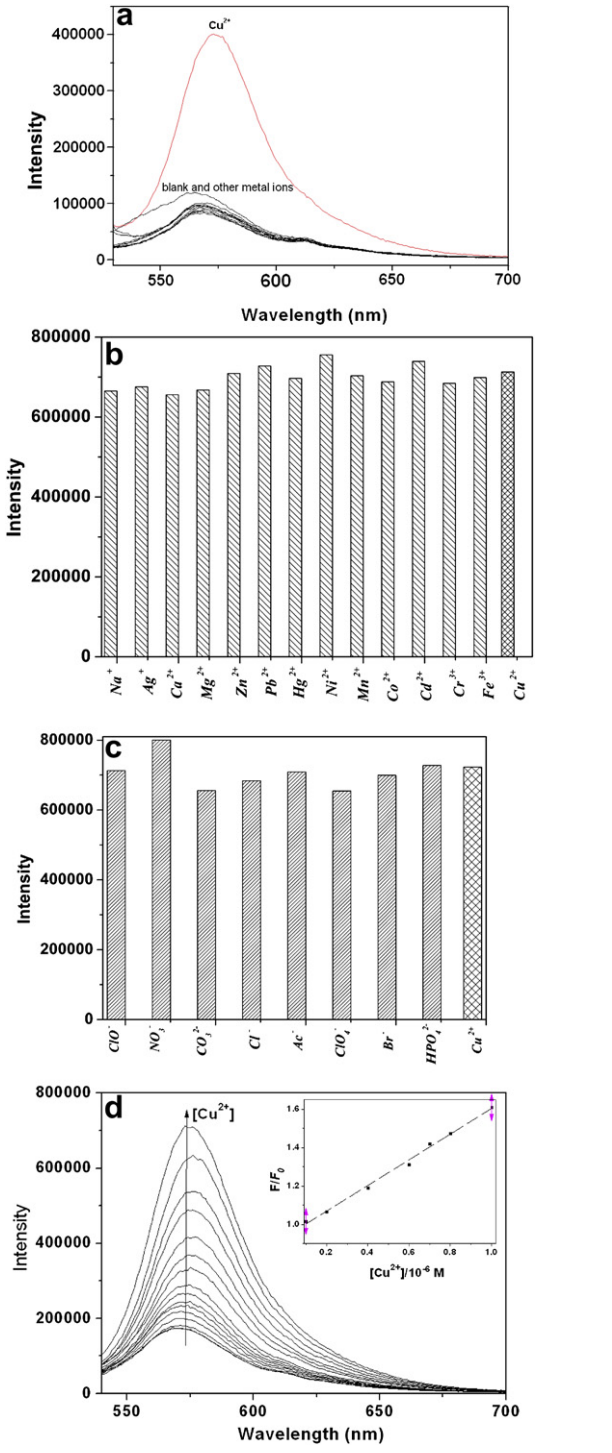

Fig. 3. (a) Fluorescence spectra of **L** (0.5 μM) with different metal ions (100 equiv.) in ethanol–water solution (6:4, v:v. 50 mM HEPES, pH 7.0). (b) Fluorescence response of **L** (1.0 μM) to 10 μM of Cu^{2+} and to the mixture of 50 μM individual other metal ions with 10 μM of Cu^{2+}. (c) Fluorescence response of **L** (1.0 μM) to 10 μM of Cu^{2+} and to the mixture of 50 μM individual anions with 10 μM of Cu^{2+}. (d) Fluorescence response of **L** (1.0 μM) with various concentrations of Cu^{2+} in ethanol–water solution (6:4, v:v. 50 mM HEPES, pH 7.0). Inset: the fluorescence at 575 nm of **L** (1.0 μM) as a function of Cu^{2+} concentrations (0.1–1 μM).

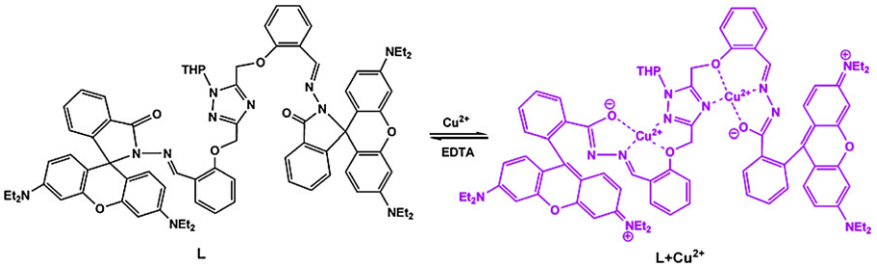

Scheme 2. Proposed binding mode between **L**/Cu^{2+}.

3. Results and discussion

3.1. The effects of pH on *L* and *L* with Cu^{2+}

The pH-control emission measurements revealed that chemosensor **L** could respond to Cu^{2+} in the pH range of 5.0–9.2 with the fluorescent intensity varying less than 10%, while the fluorescence of the free **L** can be negligible. It could be seen that the **L** facilitates quantification of the concentration of Cu^{2+} in a wide pH range (Fig. 1). Therefore, further UV–vis and fluorescent studies were carried out in ethanol–water solution (6:4, v:v, 50 mM HEPES, pH 7.0).

3.2. Uv–vis spectral response of *L*

The UV/vis of **L** to various metal ions and its selectivity for Cu^{2+} are illustrated in Fig. 2. Electronic spectra of **L** (10 μM) in ethanol–water solution (6:4, v:v, 50 mM HEPES, pH 7.0) exhibited only a very weak band above 500 nm, which could be attributed to the presence of a trace amount of the ring open form of **L**. Upon the gradual addition of Cu^{2+} up to 5 equiv., a new absorption band centered at 556 nm appeared with increasing intensity, accompanied by a clear color change from colorless to pink. This enhancement in absorbance clearly suggests the formation of the ring-opened amide form of **L** as a result of Cu^{2+} binding (Fig. 2(a)). Other metal ions, such as K^+, Ag^+, Ca^{2+}, Cd^{2+}, Co^{2+}, Cr^{3+}, Fe^{2+}, Fe^{3+}, Hg^{2+}, Mg^{2+}, Mn^{2+}, Ni^{2+} and Zn^{2+}, did not show any significant color and spectral change under identical conditions. Finally, a color change from the colorless to pink associated with the reaction of **L** with Cu^{2+} is readily detectable visually, while no significant color changes are promoted by other metal ions, as shown in inset of Fig. 2(b). Therefore **L** would serve as a "naked-eye" chemosensor targeted toward Cu^{2+}.

The method of continuous variations (Job's plot) obtained from the **L**–Cu^{2+} system in ethanol–water solution (6:4, v:v, 50 mM HEPES, pH 7.0) clearly suggested the formation of 1:2 stoichiometry between **L** and Cu^{2+} (Supporting information, Fig. S1), which is also confirmed by the Benesi–Hildebrand method [17] (Supporting information, Fig. S2).

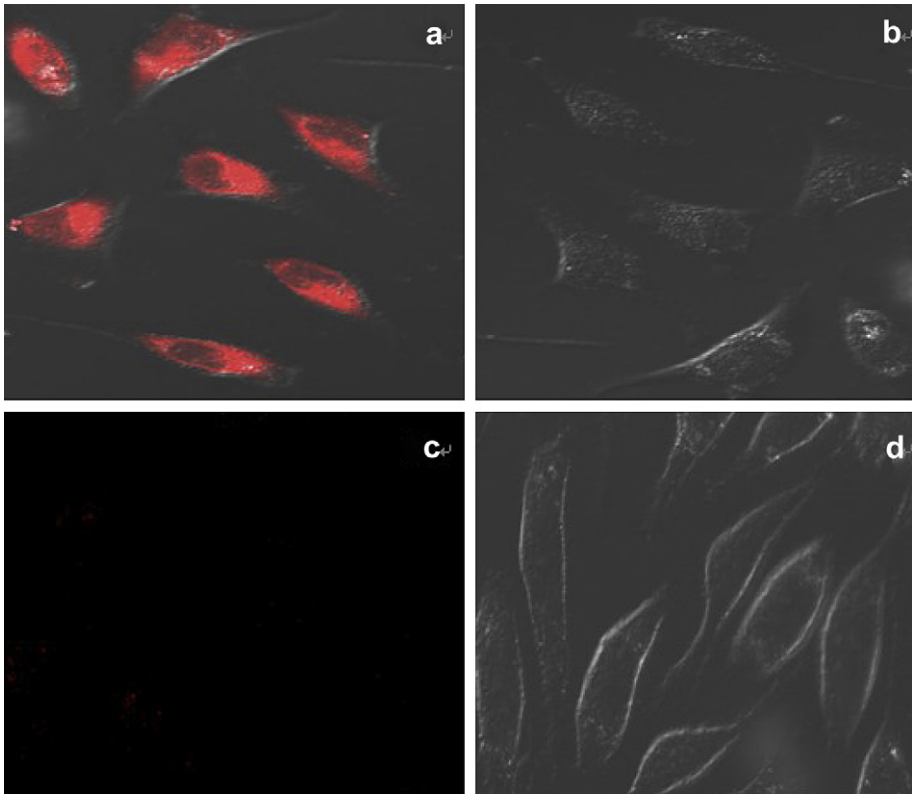

Fig. 4. Confocal fluorescence images in MCF-7 cells. (a) Cells incubated with 1 μM Cu^{2+} for 30 min, washed three times, and then further incubated with 20 μM **L** for 30 min (ex = 559 nm); (b) Bright field image of cells shown in panel (a); (c) Cells incubated with 20 μM **L** in PBS buffer for 30 min; (d) Bright field image of cells shown in panel (a).

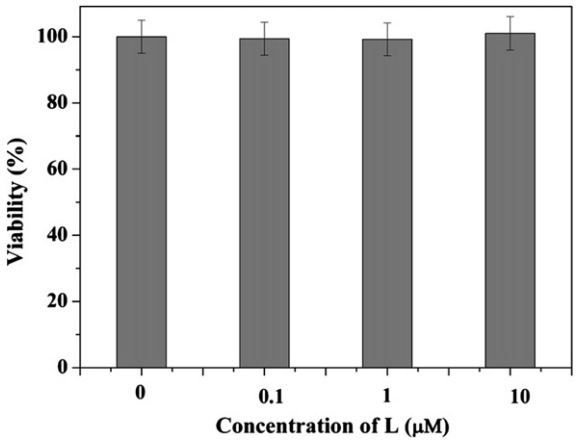

Fig. 5. Cell viability values (%) estimated by MTT proliferation test versus incubation concentrations of **L**. MCF-7 cells were cultured in the presence of 0–10 μM **L** at 37 °C.

3.3. Fluorescence spectral response of *L*

Fig. 3(a) shows the fluorescence spectra (ex = 520 nm) of **L** (0.5 μM) measured in ethanol–water solution (6:4, v:v, 50 mM HEPES, pH 7.0) with the addition of respective metal ions (100 equiv.). **L** showed only a very weak fluorescence in the absence of metal ions. The addition of Cu^{2+} resulted in remarkably enhanced fluorescence intensity (about 5-fold). Under the same condition, additions of other metal ions including Cr^{3+}, Fe^{3+}, Cd^{2+}, Na^{+}, Zn^{2+}, K^{+}, Hg^{2+}, Ag^{+}, Co^{2+}, Ni^{2+}, Pb^{2+}, Mg^{2+} and Ca^{2+} did not cause any discernible changes. These observations indicated that **L** could selectively recognize Cu^{2+} in ethanol–water solution (6:4, v:v, 50 mM HEPES, pH 7.0). For the Cu^{2+} chemosensor, cross-sensitivity to the other metal ions and to the commonly present anions was also a challenge. Therefore, competition experiments were conducted in the presence of 10 equiv of Cu^{2+} mixed with 50 equiv of other metal ions mentioned above and anions including ClO^{-}, NO_3^{-}, CO_3^{2-}, Cl^{-}, Ac^{-}, ClO_4^{-}, Br^{-} and HPO_4^{2-}, respectively. No significant variation in fluorescence intensity was found by comparison with that the same amounts of Cu^{2+} solution without other metal ions and anions (Fig. 3(b) and (c)). It is gratifying to note that all the tested metal ions and anions have no interference. To further investigate the interaction of Cu^{2+} and **L**, a fluorescence titration experiment was carried out, as shown in Fig. 3(d). A linear increase of fluorescence intensity could be observed with increasing Cu^{2+} concentration over the range of 1.0×10^{-7} M to 1.0×10^{-6} M with a detection limit of 4.5×10^{-8} M based on $3 \times \delta_{blank}/k$ (where δ_{blank} is the standard deviation of the blank solution and k is the slope of the calibration plot). The results indicated that the chemosensor **L** could sensitively detect environmentally relevant levels of Cu^{2+}.

3.4. The proposed reaction mechanism

Thus, according to the obtained results, it is very likely due to the metal ion-induced ring opening of rhodamine spirolactam, rather than other possible reactions [14]. The chemosensor is the most likely to chelate with Cu^{2+} *via* its oxygen on the salicylaldehyde, oxygen on the carbonyl group, as well as nitrogen on the hydrazine and triazole moiety (Scheme 2). On the other hand, the response of **L** to Cu^{2+} was confirmed to be reversible by the EDTA titration. Upon addition of 100 μM EDTA to the mixture of **L** (1 μM) and Cu^{2+} (10 μM) in ethanol–water solution (6:4, v:v, 50 mM HEPES, pH 7.0), the color changed from pink to almost colorless, and ~93% fluorescent emission intensity of the system was quenched (Supporting information, Fig. S3), and the EDTA replaced the receptor **L** to coordinate Cu^{2+}. When Cu^{2+} was added to the system again, the signals were almost completely reproduced, and the colorless solution turned to pink. These findings indicated that **L** can be classified as a reversible chemosensor for Cu^{2+}.

3.5. Preliminary analytical application

To further demonstrate the practical applicability of the chemosensor **L** of 1, 2, 4-triazole-linked rhodamine B to detect Cu^{2+} in living cells, the fluorescence images of MCF-7 cells were recorded before and after addition of Cu^{2+} (Fig. 4). The cells were supplemented with only **L** in the growth medium for 30 min at 37 °C, which led to very weak fluorescence as determined by laser scanning confocal microscopy (ex = 559 nm) (Fig. 4(c)). In contrast, and then loaded with 1 μM $CuCl_2$ for 30 min, a bright fluorescence was detected (Fig. 4(a)). These results suggested that chemosensor **L** can penetrate the cell membrane and might used for detecting Cu^{2+} in living cells.

To evaluate cytotoxicity of the chemosensor, **L** was taken as an example to perform a MTT assay on MCF-7 cells with dye

Table 1
Performances comparison of various fluorescent chemosensors for Cu^{2+} ion.

Modes	Reagents	Linear range, μM	LOD, μM	Testing media	Applications	Remarks	Ref.
Quenching $\lambda_{ex/em}$ = 556/603 nm	Spiropyran derivative	0.75–3.6	0.15	Ethanol or pH 6.98 (0.1 M Tris–HCl)	NA[a]	Big background fluorescence, fluorogenic change.	[4]
Enhancement $\lambda_{ex/em}$ = 510/580 nm	Rhodamine derivative	0.05–4.5	0.018	Water–ethanol (9:1, v/v, pH 7.0, 50 mM HEPES)	HeLa cells	Dual chromo- and fluorogenic changes.	[13]
Quenching $\lambda_{ex/em}$ = 600/716 nm	BODIPY derivative	NA	NA	CH_3CN containing 7% (v/v) HEPES pH 7.0	NA	NIR fluorescence, dual chemosensors for Al^{3+} and Cu^{2+}, fluorogenic change.	[18]
Enhancement $\lambda_{ex/em}$ = 328/495–616 nm	Naphthalene derivative	NA	NA	Water–CH_3CN (2:8, v/v, pH 7.2, 50 mM HEPES)	NA	Dual chromo- and fluorogenic changes, ratiometric chemosensor.	[19]
Enhancement $\lambda_{ex/em}$ = 370/450–544 nm	Naphthalimide derivative	NA	NA	CH_3CN or HEPES–CH_3CN (1:1, v/v, pH 7.4, 50 mM HEPES)	NA	Dual chromo- and fluorogenic changes, ratiometric chemosensor.	[20]
Enhancement $\lambda_{ex/em}$ = 530/570 nm	Rhodamine derivative	0–14	0.01	Water–CH_3CN (1:1, v/v, pH 7.1, 10 mM Tris–HCl)	Waster water	Dual chromo- and fluorogenic changes.	[21]
Enhancement $\lambda_{ex/em}$ = 480/554 nm	Rhodamine derivative	0–0.005	0.002	Water–CH_3CN (1:1, v/v, pH 7.2, 10 mM Tris–HCl)	EJ cells	Dual chromo- and fluorogenic changes.	[22]
Enhancement $\lambda_{ex/em}$ = 495/552 nm	Rhodamine derivative	NA	NA	Water–CH_3CN (1:1, v/v)	EJ cells	Dual chromo- and fluorogenic changes.	[23]
Enhancement $\lambda_{ex/em}$ = 510/580 nm	Rhodamine derivative	0.1–1.0	0.045	Water–ethanol (4:6, v/v, pH 7.0, 50 mM HEPES)	MCF-7 cells	Dual chromo- and fluorogenic changes.	This work

[a] NA: Not available.

concentrations from 0 μM to 10 μM. The cellular viability estimated was ca. 98% in 48 h after treatment with 10 μM of **L** (Fig. 5), exhibiting low toxicity to cultured cells.

3.6. Method performance comparison

Table 1 summarizes the photophysical properties of typical Cu^{2+} fluorescent/colorimetric chemosensors and highlights their applications. Most methods exhibit wide linear range and good selectivity, and meanwhile most of them can adopt dual chromo- and fluorogenic changes toward Cu^{2+} except some chemosensors [18,19]. Though the availability of fluorescence is increasing, there are still numerous challenges and opportunities remaining for development of new fluorophores and practical applications in biological systems, such as excitation wavelength [20,21], testing media [18,20,21]. Our newly developed chemosensor based on rhodamine derivative with 1, 2, 4-triazole as subunit presents a number of attractive analytical features such as high sensitivity, wide linear range, good selectivity and wide applicability. It can be used for rapid analysis of ultra-trace level Cu^{2+} in living cells with satisfactory results.

4. Conclusion

In summary, we describe a new chemosensor with 1, 2, 4-triazole as subunit. It selectively responds to Cu^{2+} by dual chromo- and fluorogenic changes and also facilitates "naked-eye" detection of Cu^{2+}. We believe that these observations regarding the interaction between 1, 2, 4-triazole and Cu^{2+} should serve as the platform to develop new chemosensors for other transition metal ions. In addition, we have demonstrated that the chemosensor **L** can be used to detect Cu^{2+} in living cells. It is anticipated that the chemosensor will significantly promote the studies on the effects of Cu^{2+} in biological systems.

Acknowledgments

This work was financially supported by the Research and Training Fundation of Hainan Medical University (No. HY2010-004) and the National Natural Science Foundation of China (No. 21007087).

Appendix. Supporting information

Supporting information associated with this article can be found, in the online version, at doi:10.1016/j.dyepig.2011.09.020.

References

[1] Tapiero H, Townsend DM, Tew KD. Trace elements in human physiology and pathology. Copper Biomed Pharmacother 2003;57:386–98.
[2] Lovstad RA. A kinetic study on the distribution of Cu(II)-ions between albumin and transferring. BioMetals 2004;17:111–3.
[3] Jiang P, Guo Z. Fluorescent detection of zinc in biological systems: recent development on the design of chemosensors and biosensors. Coord Chem Rev 2004;248:205–29.
[4] Shao N, Zhang Y, Cheung SM, Yang RH, Chan WH, Mo T, et al. Copper ion-selective fluorescent sensor based on the inner filter effect using a spiropyran derivative. Anal Chem 2005;77:7294–303.
[5] Kim SH, Kim JS, Park SM, Chang SK. Hg^{2+}-selective OFF–ON and Cu^{2+}-selective ON–OFF type fluoroionophore based upon cyclam. Org Lett 2006;8:371–4.
[6] Luo Y, Li Y, Lv BQ, Zhou ZD, Xiao D, Choi MMF. A new luminol derivative as a fluorescent probe for trace analysis of copper(II). Microchim Acta 2009;164:411–7.
[7] Turel M, Duerkop A, Yegorova A, Scripinets Y, Lobnik A, Samec N. Detection of nanomolar concentrations of copper(II) with a Tb-quinoline-2-one probe using luminescence quenching or luminescence decay time. Anal Chim Acta 2009;644:53–60.
[8] Mu H, Gong R, Ma Q, Sun Y, Fu E. A novel colorimetric and fluorescent chemosensor: synthesis and selective detection for Cu^{2+} and Hg^{2+}. Tetrahedron Lett 2007;48:5525–9.
[9] Lin W, Yuan L, Tan W, Feng J, Long L. Construction of fluorescent probes via protection/deprotection of functional groups: a ratiometric fluorescent probe for Cu^{2+}. Chem Eur J 2009;15:1030–5.
[10] Khatua S, Choi SH, Lee J, Huh JO, Do Y, Churchill DG. Highly selective fluorescence detection of Cu^{2+} in water by chiral dimeric Zn^{2+} complexes through direct displacement. Inorg Chem 2009;48:1799–801.
[11] Yu CW, Zhang J, Wang R, Chen LX. Highly sensitive and selective colorimetric and off–on fluorescent probe for Cu^{2+} based on rhodamine derivative. Org Biomol Chem 2010;8:5277–9.
[12] Yu CW, Zhang J, Li JH, Liu P, Wei PH, Chen LX. Fluorescent probe for copper(II) ion based on a rhodamine spirolactame derivative, and its application to fluorescent imaging in living cells. Microchim Acta 2011;174:247–55.
[13] Yu CW, Chen LX, Zhang J, Li JH, Liu P, Wang WH, et al. "Off–On" based fluorescent chemosensor for Cu^{2+} in aqueous media and living cells. Talanta 2011;85:1627–33.
[14] Kim H, Lee M, Kim H, Kim J, Yoon J. A new trend in rhodamine-based chemosensors: application of spirolactam ring-opening to sensing ions. Chem Soc Rev 2008;37:1465–72.
[15] Bradshaw JS, Nielsen RB, Tse P, Arena G, Wilson BE, Dalley NK, et al. Proton-ionizable crown compounds. 4. New macrocyclic polyether ligands containing a triazole subcyclic unit. J Heterocyclic Chem 1986;23:361–8.
[16] Yang XF, Guo XQ, Zhao YB. Development of a novel rhodamine-type fluorescent probe to determine peroxynitrite. Talanta 2002;57:883–90.
[17] Rodríguez-Cáceres MI, Agbaria RA, Warner IM. Fluorescence of metal–ligand complexes of mono- and di-substituted naphthalene derivatives. J Fluoresc 2005;15:185–90.
[18] Xie XJ, Qin Y. A dual functional near infrared fluorescent probe based on the bodipy fluorophores for selective detection of copper and aluminum ions. Sens Actuators B 2011;156:213–7.
[19] Goswami S, Sen D, Das NK. A new highly selective, ratiometric and colorimetric fluorescence sensor for Cu^{2+} with a remarkable red shift in absorption and emission spectra based on internal charge transfer. Org Lett 2010;12:856–9.
[20] Xu ZC, Han SJ, Lee C, Yoon J, Spring DR. Development of off–on fluorescent probes for heavy and transition metal ions. Chem Commun 2010;46:1679–81.
[21] Hua ZQ, Wang XM, Feng YC, Ding L, Lu HY. Sulfonyl rhodamine hydrazide: a sensitive and selective chromogenic and fluorescent chemodosimeter for copper ion in aqueous media. Dyes Pigm 2011;88:257–61.
[22] Huang L, Hou FP, Xi PX, Bai DC, Xu M, Li ZP, et al. A rhodamine-based "turn-on" fluorescent chemodosimeter for Cu^{2+} and its application in living cell imaging. J Inorg Biochem 2011;105:800–5.
[23] Liu YL, Sun Y, Du J, Lv X, Zhao Y, Chen ML, et al. Highly sensitive and selective turn-on fluorescent and chromogenic probe for Cu^{2+} and ClO^- based on a *N*-picolinyl rhodamine B-hydrazide derivative. Org Biomol Chem 2011;9:432–7.